AD-A154 332 GRAIN STRUCTURE IDENTIFICATION BY ULTRASOUND FREQUENCY AVERAGING AND DECO..(U) DREXEL UNIV PHILADELPHIA PA DEPT OF ELECTRICAL AND COMPUTER E.. 1/1

UNCLASSIFIED V L NEWHOUSE ET AL. 29 MAR 85 F/G 20/1 NL

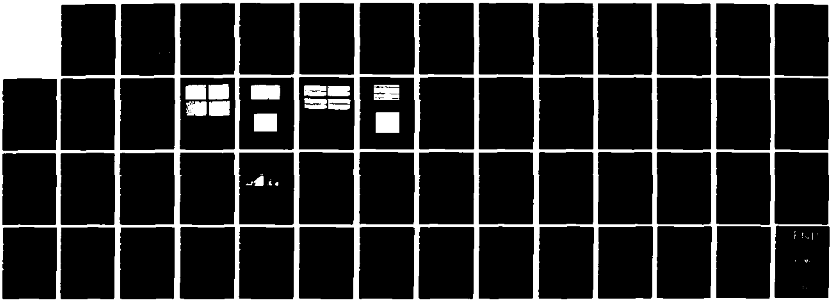

1.0 2.8 2.5

3.2 2.2

3.6

4.0 2.0

1.1

1.8

1.25 1.4 1.6

MICROCOPY RESOLUTION TEST CHART

NATIONAL BUREAU OF STANDARDS-1963-A

AFOSR-TR- 85-0469

AD-A154 332

Contract: F49620-82-K0026

Grain Structure Identification By Ultrasound Frequency Averaging and Deconvolution

Co-Authors: V.L. Newhouse, I. Amir,

S. Nash, and G. Yu

Project Director: V.L. Newhouse

Drexel University

Department of Electrical

and Computer Engineering

Philadelphia, PA 19104

Final Report for the Period

June 1, 1982 - September 30, 1984

SECURITY CLASSIFICATION OF THIS PAGE (When Data Entered)

Haou

REPORT DOCUMENTATION PAGE		READ INSTRUCTIONS BEFORE COMPLETING FORM
1. REPORT NUMBER AFOSR-TR- 85-0469	2. GOVT ACCESSION NO.	3. RECIPIENT'S CATALOG NUMBER
4. TITLE (and Subtitle) GRAIN STRUCTURE IDENTIFICATION BY ULTRASOUND FREQUENCY AVERAGING AND DECONVOLUTION		5. TYPE OF REPORT & PERIOD COVERED Final report 01 Jun 82-30 Sep 84
		6. PERFORMING ORG. REPORT NUMBER
7. AUTHOR(s) V.L.Newhouse, I Amir, S.Nash, and G. Yu		8. CONTRACT OR GRANT NUMBER(s) F49620-82-K0026
9. PERFORMING ORGANIZATION NAME AND ADDRESS Drexel University, Department of Electrical and Computer Engineering Commonwealth Hall, Philadelphia, PA 19104		10. PROGRAM ELEMENT, PROJECT, TASK AREA & WORK UNIT NUMBERS 61102F, 2306, A2
11. CONTROLLING OFFICE NAME AND ADDRESS Department of the Air Force Air Force Office of Scientific Research (AFSC)/NE Bolling Air Force Base, D.C. 20332		12. REPORT DATE March 29, 1985
		13. NUMBER OF PAGES
14. MONITORING AGENCY NAME & ADDRESS (if different from Controlling Office)		15. SECURITY CLASS. (of this report) UNCLASSIFIED
		15a. DECLASSIFICATION/DOWNGRADING SCHEDULE

16. DISTRIBUTION STATEMENT (of this Report)

Approved for public release; distribution unlimited.

17. DISTRIBUTION STATEMENT (of the abstract entered in Block 20, if different from Report)

18. SUPPLEMENTARY NOTES

19. KEY WORDS (Continue on reverse side if necessary and identify by block number)

Coherent scattering; texture characterization; spatial coherence; estimation of scatterer statistics; concentration estimation; ultrasound.

20. ABSTRACT (Continue on reverse side if necessary and identify by block number)

The goal of this research project is to measure local grain size and concentration deep in the interior of a medium ultrasonically. It will be shown that information on the scatterers' statistics can be obtained if either the field structure or the scatterer density exhibits gradients. It will be shown theoretically, and by numerical computation, that the received echo from a configuration of piston transmitter and a point receiver in the center of the piston contains a coherent component which

DD FORM 1473, 1 JAN 73 EDITION OF 1 NOV 65 IS OBSOLETE

S/N 0102-014-6601

UNCLASSIFIED

SECURITY CLASSIFICATION OF THIS PAGE (When Data Entered)

should allow concentration estimation. This report will also show theoretically and confirm experimentally that a gradient in scattering concentration will return a coherent echo from whose degree of coherence the scatterer concentration can be estimated.

We expect to apply these results soon to the estimation of grain size inside a medium.

TABLE OF CONTENTS

A. INTRODUCTION

I. Project Objectives

The goal of the research described in this report was to find techniques for estimating local values of the grain density in metallic and ceramic media, using non-destructive ultrasonic examination. Although the goal of non-destructive ultrasonic local grain size estimation deep in the interior of a medium has been a subject of widespread interest for a number of years, no technique for accomplishing this had been found at the outset of this project. The techniques for the ultrasonic determination of grain size, which are based on the variation of ultrasonic attenuation with grain size, do not permit the determination of grain size at a point inside a test sample, but merely allow the determination of the grain density averaged over the length of the sound beam from the sample surface to the interior point of measurement.

II. Research Achievements

During the period covered by this contract, it has been possible to develop a technique for analyzing backscattered echoes which has been shown to allow the determination of grain size at medium boundaries and which shows great promise of permitting grain size determination at interior points also.

The technique for surface grain size determination is based on a theory described in Section B-II which shows that the backscattered echo from an ensemble of grain-like scatterers contains both coherent and incoherent echoes, from whose ratio the surface grain density can be estimated. Section B-III describes experiments on sponges which confirm the results of the theory, and which suggest that the method should be applicable to metals and ceramics.

Section C-I extends the theory and shows that for focussed ultrasound fields of sufficiently low symmetry, illuminating grainy media, it should again be possible to obtain coherent and incoherent echoes, from whose ratio

the grain size can be determined. The section contains a calculation of the coherent echo for a specific transducer geometry which demonstrates the effect, and whose program is reproduced in the appendix (section F).

Metallurgical preparation of test specimens for this research is described in section D.

III. Conclusions

This research has introduced and provided the theoretical foundations of a novel technique for non-destructively estimating the density of scatterer ensembles from the ratio of their coherent to their incoherent ultrasonic echoes. It was shown that the coherent echoes required for this process are produced either by gradients in scatterer density, or by field foci with sufficiently low symmetry. The effectiveness of the technique for estimating surface scatterer density was demonstrated experimentally on sponges. In future research we will attempt to demonstrate that the technique using focussed beams can be used to estimate the grain density in the interior of metals and ceramics of practical importance.

B. Surface Grain Size Evaluation

I. Introduction

It is known that a uniformly illuminated infinite ensemble of random scatterers produces an incoherent echo, (defined as having zero mean at any given range delay), whose power is proportional to $\overline{N\rho^2}$. Here N is the scatterer volume density, ρ the scattering coefficient, and $\overline{}$ represents ensemble average. It has been predicted, although apparently never experimentally verified, that a coherent echo should be generated by random scatterers either when these exhibit a density gradient[1], or when they occupy a bounded region[2,3]. We have now confirmed these results by experiment and show that an estimate of the density can be extracted from the measured ratio of the coherent and incoherent echoes.

II. Theory

Let the echo detected by a sonic or electromagnetic receiver at time t after the transmission of a burst, due to a single point scatterer at $\vec{r}$ be written as

$$E_r(\vec{r},t) = \rho G(\vec{r},t) \tag{1}$$

where $G(\vec{r},t)$ is defined as the system impulse response. When many scatterers are illuminated, the echo at time t after transmission can be written

$$E(t/n) = \sum_{i=1}^{n} \rho_i G(\vec{r}_i,t) \tag{2}$$

where n is the number of scatterers in the "range cell", defined as that region of space from which echoes are received at time t after the start of transmission. We assume that this region has volume V, and that it contains n randomly positioned scatterers at locations $\vec{r}_1$, $\vec{r}_2$, $\vec{r}_3 \cdots \vec{r}_n$ of strengths ρ_1, $\rho_2 \cdots \rho_n$.

The instantaneous power at time t is

$$P(t|n) = \sum_{i}^{n} \sum_{j}^{n} \rho_i \; \rho_j \; G(\vec{r}_i,t) \; G^*(\vec{r}_j,t) \tag{3}$$

This can be separated into two parts

$$P(t|n) = \sum_{i=1}^{n} \rho_i^2 \; |G(\vec{r}_i,t)|^2 + \sum_{\substack{i \\ i \neq j}}^{n} \sum_{j}^{n} \rho_i \; \rho_j \; G(\vec{r}_i,t) \; G^*(\vec{r}_j,t) \qquad (4)$$

From eqt. (4) the average power at time t after transmission, given that there are exactly n scatterers in the range cell, can be written

$$\overline{P(t|n)} = n \; \overline{\rho_i^2 |G(\vec{r}_i,t)|^2} + n(n-1) \; \overline{\rho_i \; \rho_j \; G(\vec{r}_i,t) \; G(\vec{r}_j,t)} \qquad (5)$$

where n is the number of scatterers in range-cell volume V. Note that the average $\overline{P(t|n)}$ is on the random variable r_i and $\overline{P(t|n)}$ is the average over all possible configurations of the r_i's in the range cell. Assuming that the scattering coefficients ρ_i are uncorrelated with each other and that $\vec{r}_i$ is uncorrelated with the $\vec{r}_j$ for $i \neq j$, we can rewrite eqt. (5) as

$$\overline{P(t|n)} = n \; \overline{\rho^2} \int_V |G(\vec{r},t)|^2 \; p(\vec{r})dv + n(n-1) \; \bar{\rho}^2 \; \left| \int_V G(\vec{r},t)p(\vec{r})dv \right|^2 \quad (6)$$

where $p(\vec{r})$ is the probability of finding one individual scatterer in the volume element at $\vec{r}$, and where the integrals are taken over the volume V of the range cell. We assume the scatterers to be uniformly distributed in the range cell. So we may write

$$p(\vec{r}) = \frac{1}{V}$$

Using these two relations we can write the ensemble averaged power $\overline{P(t|n)}$

$$\overline{P(t|n)} = \frac{n}{V} \; \overline{\rho^2} \int_V |G(\vec{r},t)|^2 dv + \frac{n(n-1)}{V^2} \; \left| \int_V G(\vec{r},t)dv \right|^2 \qquad (7)$$

To find the average power $\overline{p(t)}$ we have to evaluate

$$\overline{p(t)} = \sum_{n=1}^{\infty} \overline{P(t|n)} \; p(n) \qquad (8)$$

from 7 and 8

$$\overline{p(t)} = \frac{\overline{\rho^2}}{V} \int_V |G(\vec{r},t)|^2 dv \sum_{n=1}^{\infty} np(n) + \frac{\bar{\rho}^2}{V^2} |\int_V G(\vec{r},t)dv|^2 \sum_{n=1}^{\infty} n(n-1)p(n) \quad (9)$$

where n is Poisson distributed with $\bar{n}$ as its average. Replacing

$$\sum_{n=1}^{\infty} np(n) = \bar{n}$$

and for Poisson

$$\sum_{n=1}^{\infty} n(n-1)\, p(n) = \bar{n}^2$$

we get

$$\overline{p(t)} = N\, \overline{\rho^2} \int_V |G\vec{r},t)|^2 dv + N^2\, \bar{\rho}^2\, |\int_V G(\vec{r},t)dv|^2 \quad (10)$$

$$\text{where } N = \frac{\bar{n}}{V}$$

We see that the first term on the r.h.s of eqt. (10) is proportional to $N\overline{\rho^2}$, i.e., to the average of the sum of the individual backscattered powers. We will therefore refer to it as the incoherent power P_{inc}. The second term is proportional to $(N\bar{\rho})^2$, i.e. to the square of the sum of the backscattered amplitudes. We will therefore describe it as the coherent backscattered power, P_{coh}.

We now show that P_{coh} equals the magnitude squared of the averaged echo, and that P_{inc} equals the variance of this echo.

From eqt. (2),

$$\overline{E(t)} = \sum_{n=1}^{\infty} \overline{E(t|n)}\, p(n) = N\bar{\rho} \int_V G(\vec{r},t)dv \quad (11)$$

So

$$P_{coh} = |\bar{E}|^2 = N^2\, \bar{\rho}^2\, |\int_V G(\vec{r},t)dv|^2 \quad (12)$$

The fact that P_{inc} is the variance of E(t) follows immediately, since $\sigma_E^2 = \overline{|E|^2} - |\bar{E}|^2$. Thus from eqts. (7) and (9),

$$\sigma_E^2 = P_{inc} = N\overline{\rho^2} \int_V |G(\vec{r},t)|^2 dv \tag{13}$$

Let us now examine the conditions under which the coherent backscattered echo can exist. From eqt. (7) the ratio between the coherent and incoherent echo powers is $P_{coh}/P_{inc} = NF$, where $F = \bar{\rho}^2 \, |\int G(\vec{r},t)dv|^2/\overline{\rho^2} \int |G(\vec{r},t)|^2 dv$.

For $\bar{\rho}^2/\overline{\rho^2}$ of order unity, the coherent echo will only be appreciable if both the scatterer density N and the function F are sufficiently large. To examine the magnitude of this function we start from the observation that from the definition of $G(\vec{r},t)$ given in eqt. (1), it must follow that $\int_0^\infty G(\vec{r},t)dt = 0$ since an ultrasound echo can not contain a d.c. component. We then see that although the incoherent echo power which is proportional to $\int |G(r,t)|^2 dv$ will always be greater than zero, the same is not necessarily true for the coherent power term which is proportional to $|G(r,t)dv|^2$. For instance for a plane wave travelling along the z axis, the field function can be written

$$G(\vec{r},t) = I(t-\frac{2z}{c})\, e^{i(\omega t-2kz)}$$

Thus from eqt. (9)

$$\overline{E(t)} = \bar{\rho}N \int dy \int dx \int I(t-\frac{2z}{c})e^{i(\omega t-2kz)}dz$$

which is equal to zero since $\int_0^\infty G(\vec{r},t)dt = 0$

Likewise for a point-transmitter-receiver

$$G(\vec{r},t) = [I(t-2r/c)/r^2]e^{i(\omega t-2\vec{k}\cdot\vec{r})}$$

and

$$\overline{E(t)} = \bar{\rho}N \int [I(t-2r/c)/r^2]e^{i(\omega t-2\vec{k}\cdot\vec{r})} \cdot 4\pi r^2 dr$$

which again reduces to zero. Thus we see that both for the case of plane waves and for the case of waves emitted from a point transmitter/receiver, the beam geometry has such a high degree of symmetry, that the volume integral $\int G(\vec{r},t)dv$ is found to be equal to $\int G(\vec{r},t)dt$, which has to be zero. Thus no coherent

signal exists in these two geometries for uniformly distributed scatterers.

Density Gradient

If the scatterers exhibit a certain density profile $\overline{N}(\vec{r})$, the algebra introduced earlier becomes somewhat more involved, setting $p(\vec{r})$ to be $\frac{N(r)}{\overline{n}} \cdot \frac{1}{v}$ the average power at a certain range delay t can be shown to be,

$$\overline{p(t)} = \overline{\rho^2} \int_V N(r)|G(\vec{r},t)|^2 dv + \bar{\rho}^2 \left|\int_V N(\vec{r})\ G(\vec{r},t)dv\right|^2 \tag{14}$$

with

$$E(t) = \bar{\rho} \int_V N(\vec{r})G(\vec{r},t)dv$$

we can now investigate the properties of the returned echo from the boundary between 2 regions with different scattering densities. For simplicity we assume the imaginary boundary to be planer. Replacing $\vec{r}$ by z we can write,

$$\begin{aligned} N(z) &= N_1 \qquad Z > Z_o = \frac{ct_o}{2} \\ &= N_2 \qquad Z < Z_o \end{aligned} \tag{15}$$

For a plane wave $G(z,t) = b(t-\frac{2z}{C})\exp[-i\omega(t-2z/C]$; and the returned echo from the boundary becomes

$$\overline{E(t_o)} = N_1\ \overline{\rho_1} \int_{-\infty}^{o} b(t)\exp[-\omega t]dt + N_2\ \overline{\rho_2} \int_{o}^{\infty} b(t)\exp[-\omega t)dt \tag{16}$$

$\overline{\rho_1}$ and $\overline{\rho_2}$ are the reflection coefficients of the scatterers in region 1 and 2 respectively. Note that the volume integral in 14 becomes a time integral by change of variables. If the range cell is situated such that the boundary is closely in its center, the variance of $E(t_o)$ can be shown to be,

$$\sigma^2 \cong \frac{1}{2}[\sigma_1^2 + \sigma_2^2] = [N_1\overline{\rho_1^2} + N_2\overline{\rho_2^2}] \int_o^{\infty} |b(t)|^2 dt \tag{17}$$

where σ_1^2 and σ_2^2 are the variances of the returned echo from region 1 and region 2 respectively.

III. Experimental Results

According to the results obtained earlier we should be able to observe a coherent effect from an echo returned from the boundary between 2 different scattering density regions.

One of the easiest ways to obtain scatterers immersed in water and have a sharp boundary is to use sponges. The sponge can be cut to produce a sharp boundary. The sponge is then immersed in water and the complex structure of the sponge fibers can be considered as randomly distributed scatterers immersed in water. Furthermore, we can clamp together two sponges with different scattering properties and compose a sharp boundary between 2 different media, or we can use only one sponge for which we have 2 media with $N_1=0$ in region 1 and N_2 in region 2. Figs. 1a-1d show pictures of sponges used in the experiments. One can see that sponge A has the finest grain structure, sponge B has a larger honeycomb structure, sponge C is more dilute, and sponge D is very dilute in comparison to sponges A, B and C. In fig. 2 we see sponges B and C side by side. One can see that the boundary is sharp in comparison to a wavelength (frequency of 2.25 MHz). One can also see again that the honeycomb structure of sponge B is finer than that of sponge C. In fig. 3 we see the echo returned from sponge A. One can see that the echo from the boundary is highly coherent, i.e., the echoes do not change phase and are not as random in comparison to the echo from inside the sponge. These echoes are incoherent in the sense that for a certain range delay the amplitude is random with zero mean.* From the theory introduced earlier we know that the ratio between the average echo squared from

*Note that the echoes from close vicinity to the first echo are somewhat weaker than the echoes from the echoes deep inside the sponge (eventually the echoes are weakening due to attenuation). The reason stems from the fact that the transducer surface is not perfectly parallel to the sponge surface and thus it takes more time for the incoherent term to fully develop. The slight angle change has practically no effect on the coherent term magnitude. So the estimation of the incoherent term should be done further away from the first echo.

the boundary and the average power from inside the sponge, neglecting attenuation, is proportional to the scattering density. So, practically, one can estimate the sponge density from the results obtained. We will not attempt here to estimate the sponge density, but will show qualitatively that the experimental results behave according to the theory. Figs. 4A,B,C, and D represent the echoes received from sponges A, B, C, and D respectively. Each of the pictures is composed of four pictures, one on top of the other, from four different locations in the sponge, with identical distances from the transducer to the sponge. Fig. 4A is similar to fig. 3, with the traces one on top of the other. One can see that the coherent component of the echo from the boundary is relatively large in comparison to the echo returned from within the sponge. Sponge D, with the largest honeycomb structure, has practically zero coherent effect. The honeycomb structure of sponges B and C is similar in shape, so we can assume that $\bar{\rho}^2/\overline{\rho^2}$ is also similar. The integrals in eqt. 10 are also similar for the two sponges, as they involve only transducer parameters, which were the same for the experiments. So the ratio between the coherent power term and the incoherent term should be proportional to the scattering density. Evaluating the coherent term from the average of the first echo from the boundary and the power from inside the sponge (the incoherent term), we get NF to be about 2.1 from sponge B and about 0.8 from sponge C, which implies a density ratio of about 2.6. The actual scattering density ratio that can roughly be established from the micrographs is about 2.2, which is in close agreement, considering the fact that we used only four sample points and no special arrangements for producing extremely smooth surface and keeping the sponge surface parallel to the transducer surface. Sponge D has much lower density, too low to establish a coherent term out of only 4 sample points. In fig. 5 the echo from sponge D clamped to sponge B is shown. The coherent effect is clearly seen along the center vertical line of the picture. We investigated also the

angle dependence of the reflected echo. The sponge under test was chosen to be sponge B. One can see in fig. 6 that the coherent effect is highly angle-sensitive, while the echo reflected from within the sponge is not angle-dependent. The behavior of the coherent component is very much like specular reflection (not proved in this report); thus its behavior resembles specular reflection. The reflection from within the sponge is independent of the angle as the echo is independent of the boundary region.

Conclusions

We have pointed out earlier that since neither an electromagnetic nor an acoustic transducer can transmit d.c. signals, the time integral of all transmitted electromagnetic or acoustic signal amplitudes is zero. This implies that the echoes of such signals from constant density random scatterers are purely incoherent for either a plane wave or a point source emitter/receiver. In the presence of strong density gradients, however, such as those which occur near a boundary, we have demonstrated the existence of coherent echo components, defined as echoes with a finite ensemble average at a specific range delay. Measuring the ratio between the coherent echo and the echo variance should permit estimation of the quantity $N\bar{\rho}^2/\bar{\rho}^2$, which in the case of metals, for example, is related to the grain size.

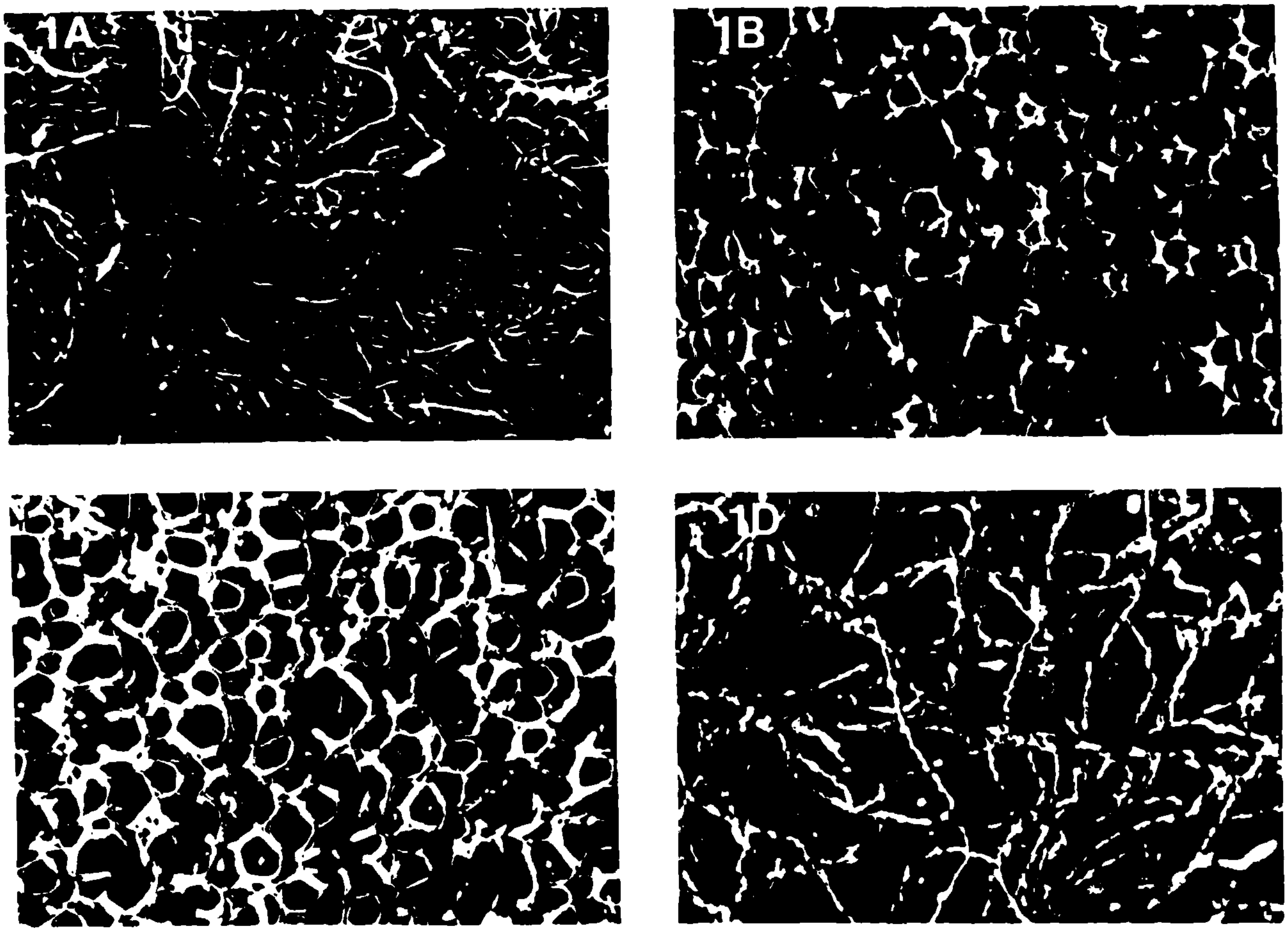

Fig. 1. A photograph of the surfaces of sponges A,B,C and D. The fine honeycomb structure is visible. (The width of each picture corresponds to 6.5 mm.)

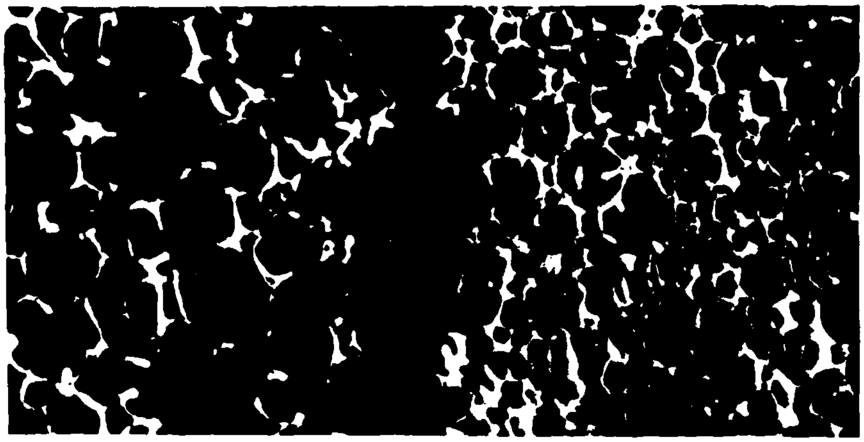

Fig. 2. Sponges B and C side by side. It is seen that the honeycomb structure of sponge B is finer than that of sponge C.

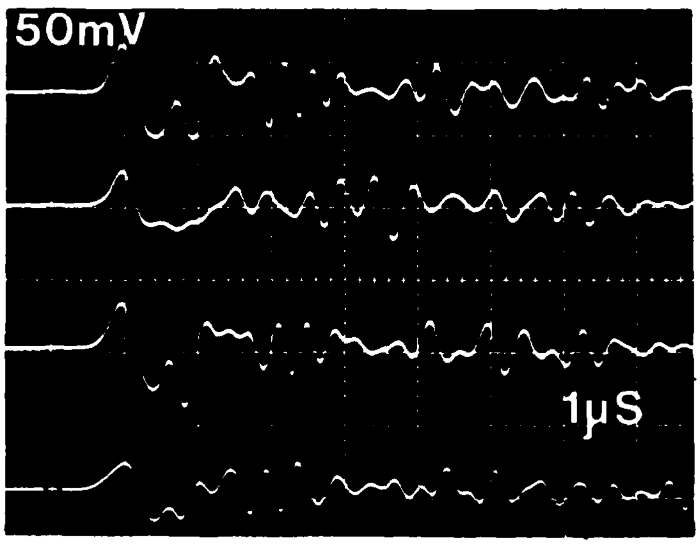

Fig. 3. Four different echoes from sponge B. Note the coherent echo component from the sponge boundary and the incoherent component from within the sponge.

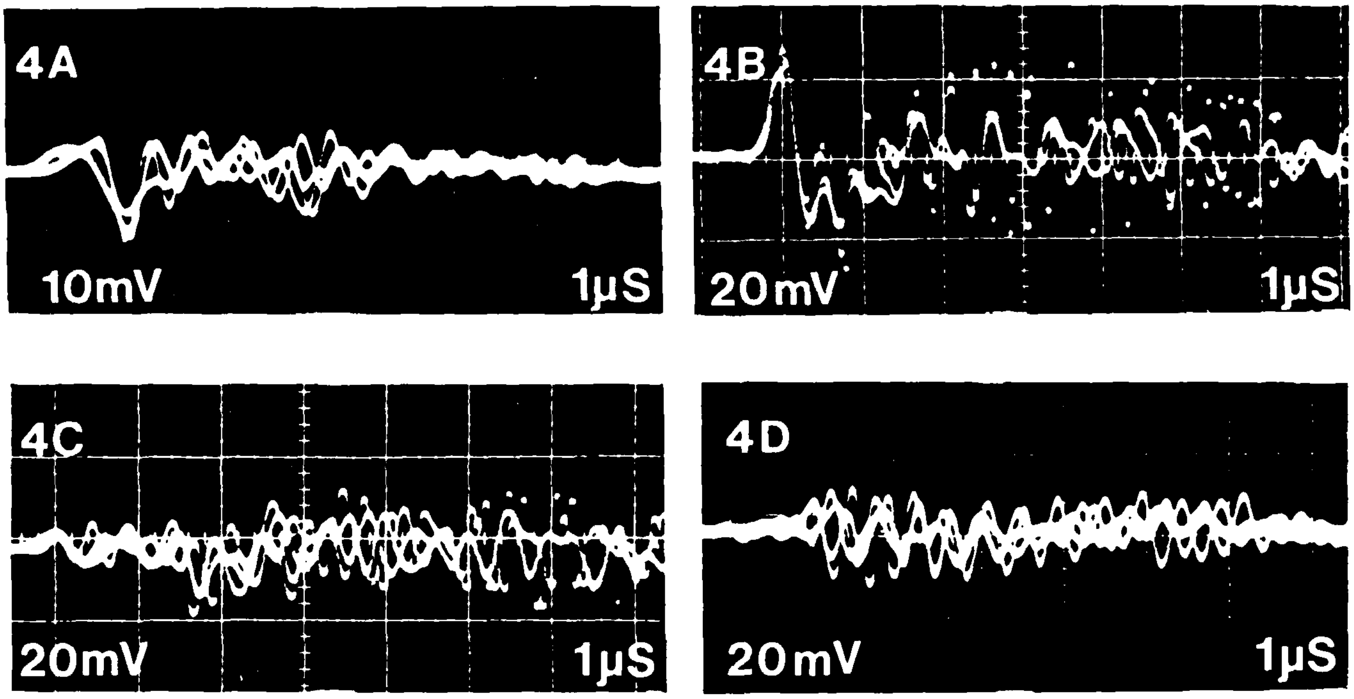

Fig. 4a. Four traces (one on top of the other) of the reflected echo from sponge A. Note the large coherent component of the echo from the boundary.

Fig. 4b. Sponge B. Note that the coherent component is not as large in comparison to the echo from within the sponge as for fig. 4A.

Fig. 4c. Sponge C. Note that the coherent component is smaller in comparison to the echo from within the sponge than in fig. 4B.

Fig. 4d. Sponge D. The coherent component was found to be negligible in repetitive experiments.

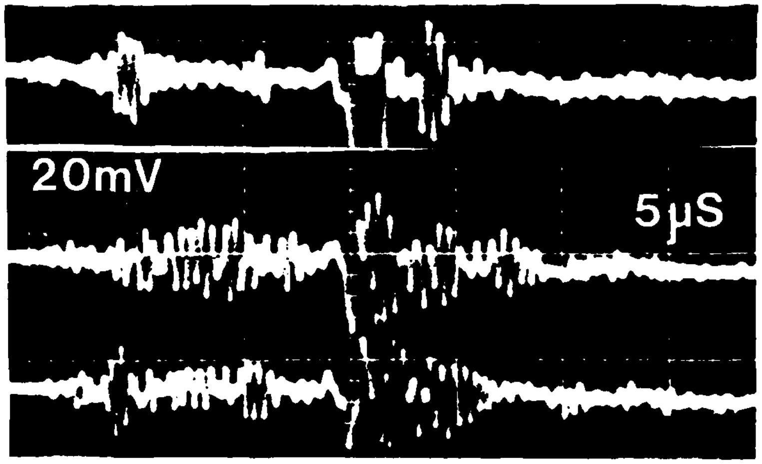

Fig. 5. The received echo from a 2 layer sponge complex composed of sponges C and B. The coherent component can be seen on the central vertical line. Also note that the power reflected from sponge C is less than that reflected from sponge B.

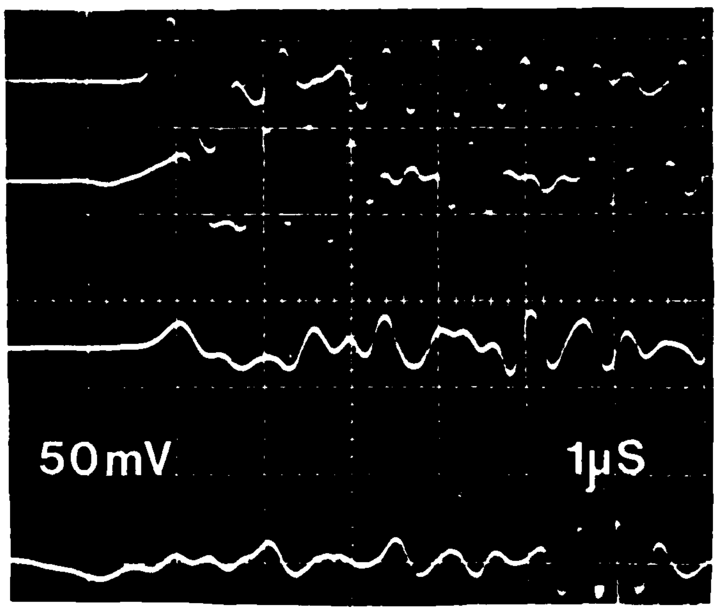

Fig. 6. Angle dependence of the coherent component (sponge B). Note that while the coherent term is highly sensitive to angle variations, the echo from within the sponge is angle insensitive.

C. Internal Grain Size Evaluation

I. Introduction

The technique introduced in the last chapter enables us to estimate the scattering density near a boundary, or when a sharp scattering density exists. However, if we need to estimate uniform scattering density inside the metal, this technique would clearly fail. However, if we introduce a sharp field gradient in the range of interest, a coherent echo will still be generated, as can be learned from eqt. (10) of the preceding chapter. In this section we investigate the coherent echo created by a field gradient expected from a simple geometry of transmitter/receiver. The transmitter is a circular disk, and the receiver is a point transducer at its center. We show that the configuration leads to a coherent echo from a half-space filled with inhomogeneities.

II. Field Requirements for Coherence

Let us now examine the conditions under which the coherent backscattered echo can exist. From eqt. (7) the ratio between the coherent and incoherent echo powers is $P_{coh}/P_{inc} = NF\ \bar{\rho}^2/\rho^2$, where $F = \dfrac{|\int G(\vec{r},t)dv|^2}{\int |G(\vec{r},t)|^2 dv}$

Since $\bar{\rho}^2/\overline{\rho^2}$ is usually of order unity, the coherent echo will be appreciable only if both the scatterer density N and the function F are sufficiently large. To examine the magnitude of this function, we start from the observation that from the definition of $G(\underline{\vec{r}},t)$ given in eqt. (1), it must follow that $\int_0^\infty G(\vec{r},t)dt = 0$, since an ultrasound echo can not contain a d.c. component. We see therefore that although the incoherent echo power which is proportional to $\int |G(\vec{r},t)|^2\ p(\vec{r})dv$ will always be greater than zero, the same is not necessarily true for the coherent power term which is proportional to $|\int G(\vec{r},t)p(\vec{r})dv|^2$. For instance for a plane wave travelling along the z axis, the field function can be written

$$G(\vec{r},t) = I(t-2z/c)e^{i(\omega t-2kz)}$$

Thus from eqt. (8)

$$\overline{E(t)} = \bar{\rho}N \int dy \int dx \int_{\infty} I(t-2\tfrac{z}{c})e^{i(\omega t-2kz)}dz$$

which is equal to zero since $\int_0 G(\vec{r},t)dt = 0$.

Likewise for a point transmitter-receiver

$$G(\vec{r},t) = [I(t-2r/c)/r^2]e^{i(\omega t-2\vec{k}\cdot\vec{r})}$$

and

$$\overline{E(t)} = \bar{\rho}N \int_0 [I(t-2r/c)/r^2]e^{i(\omega t-2\vec{k}\cdot\vec{r})} \cdot 4\pi r^2 dr$$

which again reduces to zero. Thus we see that both for the case of plane waves and for the case of waves emitted from a point transmitter/receiver, the beam geometry has such a high degree of symmetry that the volume integral $\int G(\vec{r},t)dv$ is found to be equal to $\int G(\vec{r},t)dt$ which has to be zero. Thus no coherent signal exists in these two geometries for uniformly distributed scatterers.

The above calculations suggest that a non-zero coherent echo would be produced with separate transmitters and receivers, preferably having opposite magnitudes of field gradient in the region of maximum intensity. Such a geometry would be provided, for example, by a focussed transmitter/point receiver pair. For reasons of computational simplicity we have chosen to examine the case of an unfocussed flat circular piston transmitter set in a rigid baffle, with a point receiver at its center, (see Fig. 7). For this type of transmitter Arditi et al[4] have shown that for a velocity normal to the transducer face v(t), the transmitted sound pressure at point $\underline{r}$ can be written

$$p(\vec{r},t) = -\ \varepsilon\ \partial v/\partial t * h_t(\vec{r},t) \qquad (11)$$

where ε is the density of the medium and the transmitter impulse response is

$$h_t(\vec{r},t) = 1/2\pi \int_S \delta(t - r'/c)/r'\ dS$$

which has been calculated for the flat disk piston transducer in a rigid baffle by Oberhettinger[5].

The echo due to a single scatterer at $\underline{r}$ for which ρ is unity, can then be written

$$G(\vec{r},t) = p(\vec{r},t) * h_r(\vec{r},t) \tag{12}$$

where $h_r(\vec{r},t)$ is the receiver impulse response which for a point receiver at the origin becomes

$$h_r(\vec{r},t) = \delta(t - r/c)/2\pi r \tag{13}$$

Combining Eqts. (11), (12) and (13) gives for the echo of a single scatterer at $\vec{r}$,

$$G(\vec{r},t) = - \varepsilon/2\pi \ \partial v/\partial t * [1/r \ h_t(\vec{r}, t - r/c)] \tag{14}$$

which reduces to $G_\delta(\vec{r},t) = - \varepsilon/(2\pi r)h_t(\vec{r}, t - r/c)$ if $\partial v/\partial t$ is taken to be an impulse at time zero.

Integrating $G_\delta(\vec{r},t)$ over space provides us, as shown by Eq. (8) with the spatially averaged coherent echo $\overline{E_\delta(t)}$ resulting from $\partial v/\partial t = \delta(t)$ for uniform average density scatterers for which ρn is unity. This integral is plotted in Fig. 8 for $t > a/c$. It can be seen that as t approaches infinity $\overline{E_\delta(t)}$ approaches the constant $a^2c/4\pi$, which corresponds to the echo that would be obtained from a point source/receiver of strength a^2, illuminating a half space. By analysing the case of a point source in an <u>infinite</u> plane, it can be shown that near the origin $\overline{E_\delta(t)} \to c^3/4 \ t^2$ corresponding to the analytically obtainable solution for an infinite area transmitting transducer.

For a transducer acceleration $\dot{v}(t)$ of finite length, the spatially averaged coherent echo will be given by

$$\overline{E(t)} = \dot{v}(t) * \overline{E_\delta(t)} \ . \tag{15}$$

This quantity has been calculated for a transducer surface displacement consisting of m sinusoids i.e. for $\mu = \sin \omega t$ for $0 < t < 2\pi m/\omega$, where m is an integer, and with the simiplifying assumption that we can represent the spatially averaged coherent echo $\overline{E_\delta(t)}$ resulting from impulse acceleration and shown in Fig. 8, as

$$\overline{E_\delta(t)} = a^2[K\, e^{-\alpha t/a} + \frac{c}{4\pi}] \text{ for } t > a/c \tag{16}$$

with $K = 30{,}000$ cm/sec and $\alpha/a = 5000$Hz.

Substituting eq. (16) into eq. (15) gives, after some higher algebra,

$$\overline{E(t)} = \frac{a^2K\,\omega^3}{(\alpha/a)^2+\omega^2}\,[1 - e^{\frac{2m\pi\alpha}{a\omega}}]\, e^{-(\alpha/a)t} \text{ for } t > \frac{a}{c} > \frac{2\pi m}{\omega}\,. \tag{17}$$

We see that for the geometry analyzed here, of a disk/point-source transducer pair, the maximum coherent echo occurs immediately after the end of the transmitted signal and therefore comes from a region close to the point detector, where the field is maximum. If the disk were replaced with a focussed transducer the maximum coherent echo would be expected to come from the focal region which is at a distance from the tranducers.

We see also that the decay time constant of $\overline{E_\delta(t)}$, $a/\alpha = (5000)^{-1}$ secs is just 12 times longer than the sound transit time $2a/c$ across a disk transducer diameter. Thus to maintain the frequency of this signal high enough to be within the passband of the transducers used, the diameter of the disk must be kept as small as possible. Since a point source does not have a good low frequency response, this should be used as the transmitter rather than the receiver. Using a focussed element instead of the disk will probably also help to increase the frequency of $\overline{E_\delta(t)}$.

III. Discussion

As pointed out earlier, since neither an electro-magnetic nor an acoustic transducer can transmit a d.c. signal, the time integral of all transmitted electromagnetic or acoustic signal amplitudes is zero. Using this fact, we showed that the echoes of such signals from constant density random scatterers, with attenuation neglected, are purely incoherent for either a plane wave or a point source/emitter/receiver (i.e., E(t) has a time average of zero when the scatterers move with respect to the transducer). In the presence of strong field gradients of sufficiently low symmetry, however, such as those produced by tranducer pairs, we predict the existence of coherent echo components, defined as echoes with a finite ensemble average.

As shown by eqt. (7) the ratio between the coherent and incoherent echo powers is

$$\frac{P_{coh}}{P_{inc}} = N \, \frac{\bar{\rho}^2 \left| \int G(r,t) dv \right|^2}{\overline{\rho^2} \int \left| G(r,t) \right|^2 dv}$$

If the coherent echo comes mainly from a limited region such as a transducer focus, then a measurement of the ratio P_{coh}/P_{inc} should enable the local value of $N\bar{\rho}^2/\overline{\rho^2}$ to be estimated when the field function is known. This should be applicable to the estimation of grain size in metals, and possibly to tissue characterization.

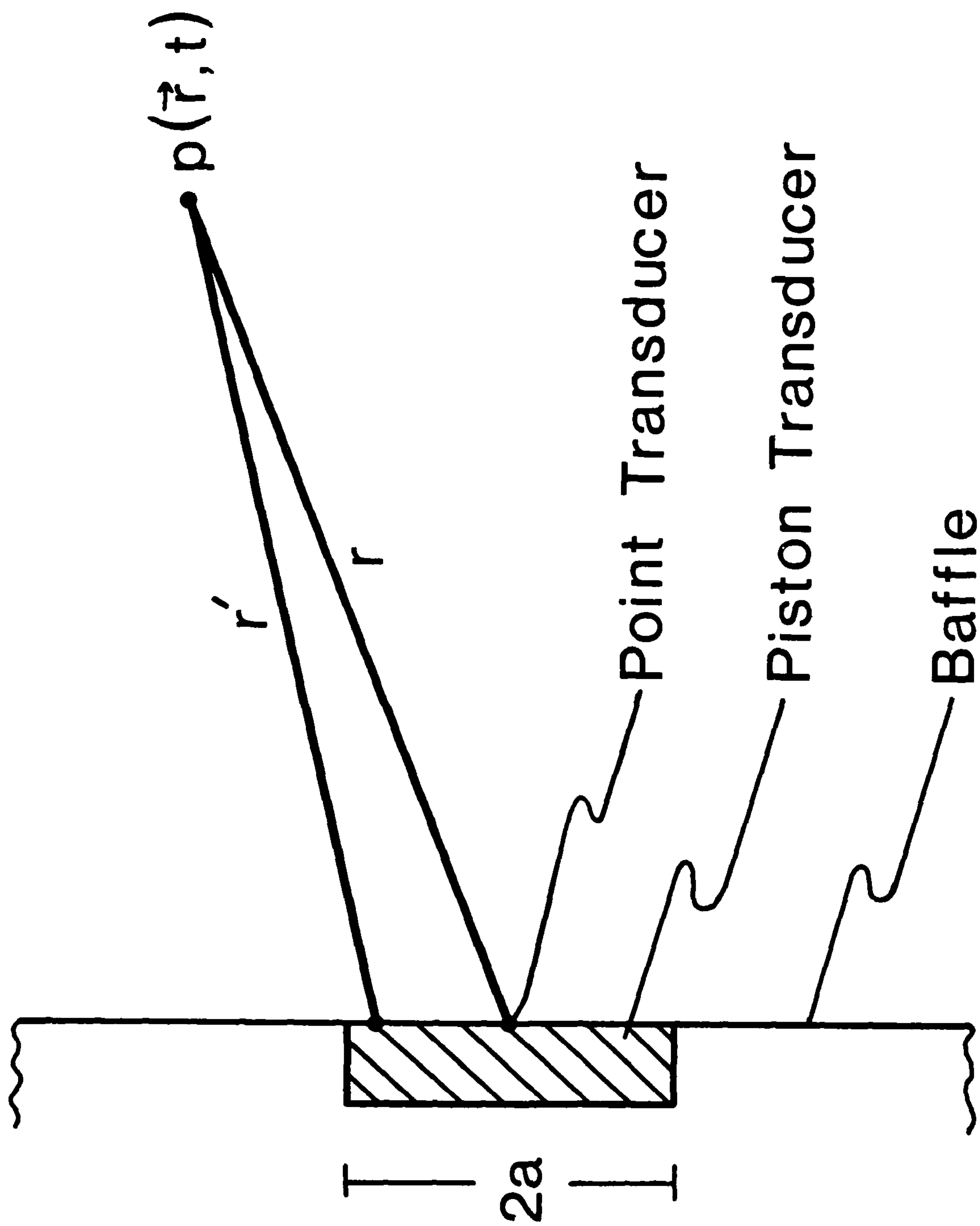

Figure 7. Circular piston transducer set in rigid baffle with point transducer at center.

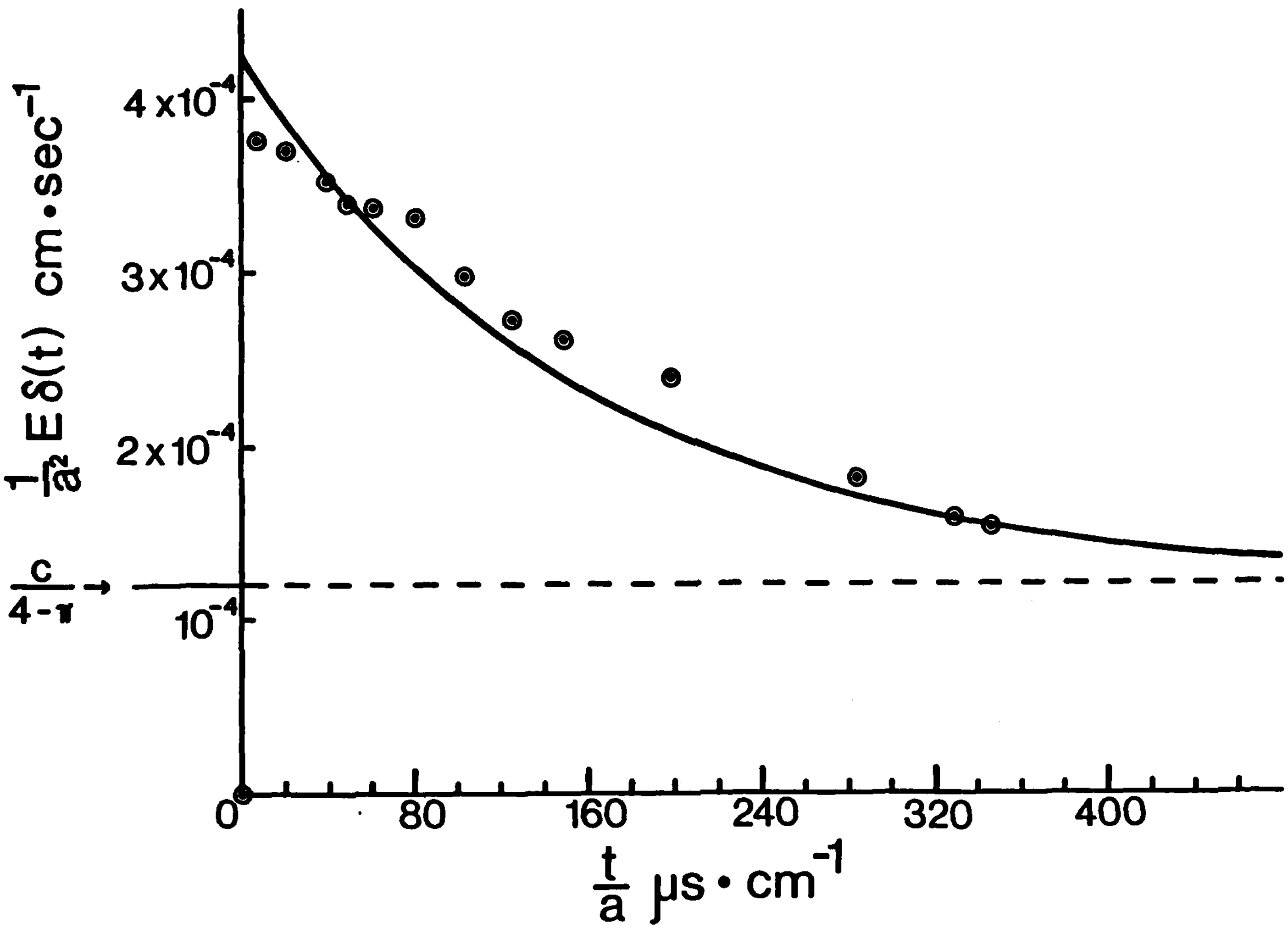

Figure 8. Echo $E\delta(t)$ received from a uniform scattering medium by the piston/point transducer pair of Figure 7 for impulse acceleration of the piston surface at time zero.

D. Metallurgical Sample Preparation

SPECIMEN PREPARATION

Test specimens suitable for this investigation should be capable of rendering an unambiguous ultrasonic signal from fine, uniformly distributed microconstituents. A graded series of specimens should contain such entities in sizes ranging in diameter from 25-150 μm.* Physically, the specimen test faces should be parallel and spaced not less than 50 mm apart.

HIGH PURITY IRON

A hot-forged bar of high purity iron was selected as the first candidate material for test specimens. The bar was large enough (about 75 mm in diameter) and, by virtue of its composition, should have had a microstructure consisting only of equiaxed grains. That in fact turned out to be so, with one important exception: the grain size of the iron, shown in Figure 9, was huge and much too large for the intended use. Nevertheless the attributes of this material made it worthwhile to see if it could be altered and saved.

The ferrite grain size of iron may be modified - increased or decreased - through appropriate heat treatment. The heat treatment consists of repeated cycles of rapid heating to 35°C above the austenitic transformation temperature (910°C), holding until the center of the specimen reaches temperature, then quenching in water to reform ferrite grains. This treatment sequence was applied to one-centimeter cubes ten times, with the results shown in Figure 10. Clearly a large reduction in grain size was achieved; however, the grains are not of uniform size, and some remain quite large. It is questionable therefore whether specimens having such a microstructure would be suitable for the purpose of this investigation.

---

*Equiaxed metallic grains in this range of diameters correspond to standard ASTM grain size numbers between 7.5 and 2.5. Refer to the attached Table of Micro-Grain Size and Grain Size Charts.

Commercial Purity Cast Aluminum

While work on modifying the grain structure of the high-purity iron was in progress, a quantity of commercially pure (i.e., 1100) aluminum was obtained from Alcoa. The ingot was cast by the D.C. process and refined with a titanium-boron grain refining addition. Commercial purity (1100) aluminum contains small quantities of iron and silicon as the principal impurity elements. Iron/silicon precipitates appear as black particles in the dendritic microstructure shown in Figure 11. This material may prove to be useful for making specimens; its micro-constituents are closely spaced and uniformly distributed.

Contingent Material

In the event that neither the commercially pure aluminum nor high-purity iron yields satisfactory specimen material, it will become necessary to place a special order. That situation has the advantage of our being able to specify precisely both the physical dimensions and requisite microstructure of the material as conditions of purchase.

Figure 9. Pure Iron As Forged. 100X

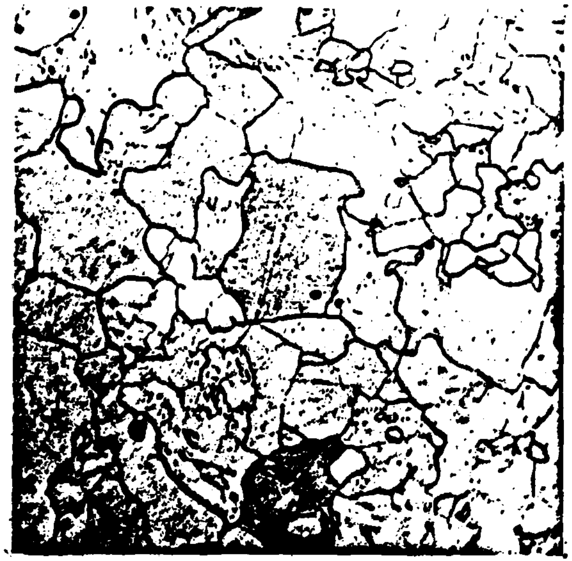

Figure 10. Pure Iron After Cyclic Grain Refining Heat Treatment. 100X

Figure 11. DC Cast 1100 Aluminum Grain Refined. 100X

TABLE I. Grain Size Relationships

ASTM Micro-Grain Size Number	Calculated "Diameter" of Average Grain		Average Intercept Distance[b]		Calculated Area of Average Grain Section		Average Number of Grains per cu mm	Nominal Grains per sq mm at 1 ×	Nominal Grains per sq. in. at 100 ×
	mm	in.	mm	in.	sq mm	sq in.			
		$\times 10^{-3}$		$\times 10^{-3}$	$\times 10^{-3}$	$\times 10^{-6}$			
00[a]	0.508	20.0	0.451	17.8	258	400	7.63	3.88	0.250
0	0.359	14.1	0.319	12.6	129	200	21.6	7.75	0.50
0.5	0.302	11.9	0.268	10.6	91.2	141	36.3	11.0	0.707
1.0	0.254	10.0	0.226	8.88	64.5	100	61.0	15.5	1.0
...	0.250	9.84	0.222	8.74	62.5	96.9	64.0	16.0	1.03
1.5	0.214	8.41	0.190	7.47	45.6	70.7	103	21.9	1.41
....	0.200	7.87	0.178	6.99	40.0	62.0	125	25.0	1.61
....	0.180	7.09	0.160	6.29	32.4	50.2	171	30.9	1.99
2.0	0.180	7.07	0.160	6.28	32.3	50.0	172.3	31.0	2.0
2.5	0.151	5.95	0.134	5.30	22.8	35.4	290	43.8	2.83
....	0.150	5.91	0.133	5.24	22.5	34.9	296	44.4	2.87
3.0	0.127	5.00	0.113	4.44	16.1	25.0	488	62.0	4.0
....	0.120	4.72	0.107	4.20	14.4	22.3	578.9	69.4	4.48
3.5	0.107	4.20	0.0948	3.73	11.4	17.7	821	87.7	5.66
...	0.900	3.54	0.0799	3.15	8.10	12.6	1 370	123	7.97
4.0	0.0898	3.54	0.0797	3.14	8.06	12.5	1 380	124	8.0
4.5	0.076	2.97	0.0671	2.64	5.70	8.84	2 320	175	11.3
...	0.070	2.76	0.0622	2.45	4.90	7.59	2 920	204	13.2
5.0	0.064	2.50	0.0564	2.22	4.03	6.25	3 910	248	16.0
....	0.060	2.36	0.0533	2.10	3.60	5.58	4 630	278	17.9
5.5	0.0534	2.10	0.0474	1.87	2.85	4.42	6 570	351	22.6
....	0.050	1.97	0.0444	1.75	2.50	3.88	8 000	400	25.8
6.0	0.045	1.77	0.0399	1.57	2.02	3.13	11 000	496	32.0
...	0.040	1.58	0.0355	1.40	1.60	2.48	15 600	625	40.3
6.5	0.038	1.49	0.0335	1.32	1.43	2.21	18 600	701	45.3
....	0.035	1.38	0.0311	1.22	1.23	1.90	23 000	816	52.7
7.0	0.032	1.25	0.0282	1.11	1.01	1.56	31 000	992	64.0
...	0.030	1.18	0.0267	1.05	0.90	1.40	37 000	1 110	71.7
7.5	0.027	1.05	0.0237	0.933	0.713	1.10	52 500	1 400	90.5
...	0.025	0.984	0.0222	0.874	0.625	0.969	64 000	1 600	103
8.0	0.0224	0.884	0.0199	0.785	0.504	0.781	88 400	1 980	128
....	0.0200	0.787	0.0178	0.699	0.40	0.620	125 000	2 500	161
8.5	0.0189	0.743	0.0168	0.660	0.356	0.552	149 000	2 810	181
9.0	0.0159	0.625	0.0141	0.555	0.252	0.391	250 000	3 970	256
....	0.0150	0.591	0.0133	0.524	0.225	0.349	296 000	4 440	287
9.5	0.0134	0.526	0.0119	0.467	0.178	0.276	420 000	5 610	362
10.0	0.0112	0.442	0.00997	0.392	0.126	0.195	707 000	7 940	512
....	0.0100	0.394	0.00888	0.350	0.10	0.155	1.00×10^6	10 000	645
10.5	0.00944	0.372	0.00838	0.330	0.089	0.138	1.19×10^6	11 200	724
...	0.00900	0.354	0.00799	0.315	0.081	0.126	1.37×10^6	12 300	797
....	0.00800	0.315	0.00710	0.280	0.064	0.0992	1.95×10^6	15 600	1 010
11.0	0.00794	0.313	0.00705	0.278	0.063	0.0977	2.00×10^6	15 900	1 020
...	0.00700	0.276	0.00622	0.245	0.049	0.0760	2.92×10^6	20 400	1 320
11.5	0.00667	0.263	0.00593	0.233	0.045	0.0691	3.36×10^6	22 400	1 450
....	0.00600	0.236	0.00533	0.210	0.036	0.0558	4.63×10^6	27 800	1 790
12.0	0.00561	0.221	0.00498	0.196	0.031	0.0488	5.66×10^6	31 700	2 050
....	0.00500	0.197	0.00444	0.175	0.025	0.0388	8.00×10^6	40 000	2 580
12.5	0.00472	0.186	0.00419	0.165	0.022	0.0345	9.51×10^6	44 900	2 900
....	0.00400	0.158	0.00355	0.140	0.0160	0.0248	15.62×10^6	62 500	4 030
13.0	0.00397	0.156	0.00352	0.139	0.0158	0.0244	16.0×10^6	63 500	4 100
13.5	0.00334	0.131	0.00296	0.117	0.011	0.0173	26.9×10^6	89 800	5 800
...	0.00300	0.118	0.00266	0.105	0.009	0.0140	37.0×10^6	111 000	7 170
14.0	0.00281	0.111	0.00249	0.0981	0.0079	0.0122	45.2×10^6	127 000	8 200
....	0.00250	0.098	0.00222	0.0874	0.00625	0.00969	64.0×10^6	160 000	10 300

[a]The use of 00 is recommended instead of "—1" or "minus 1" to avoid confusion.
[b]Value of Heyn intercept for equiaxed grains.
[c]From: Designation E-112, ASTM Standards, 1961, Part 3—Metal Test Methods; published by American Society for Testing and Materials,Philadelphia, Pa.

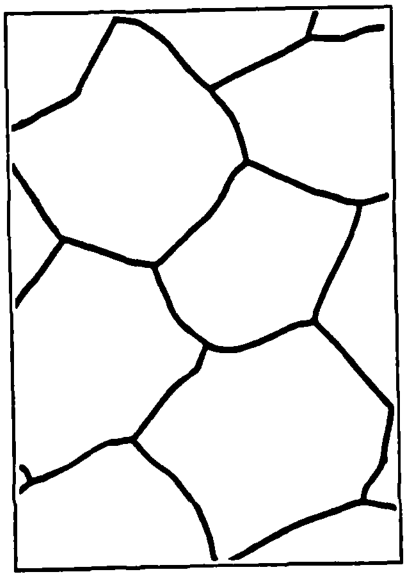

Grain Size No. 1

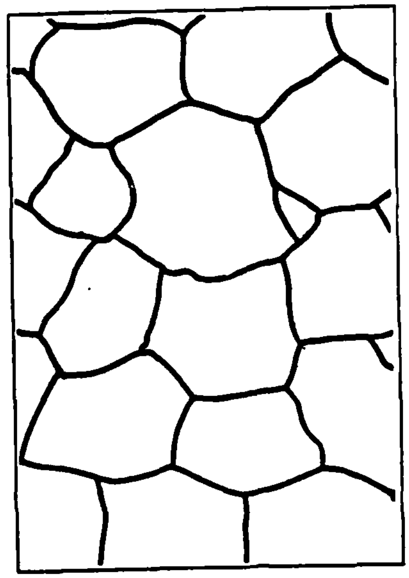

Grain Size No. 2

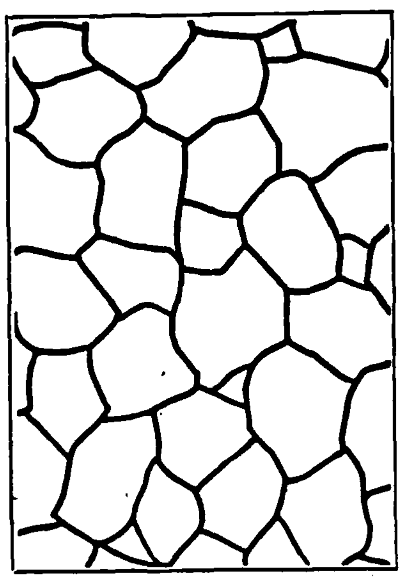

Grain Size No. 3

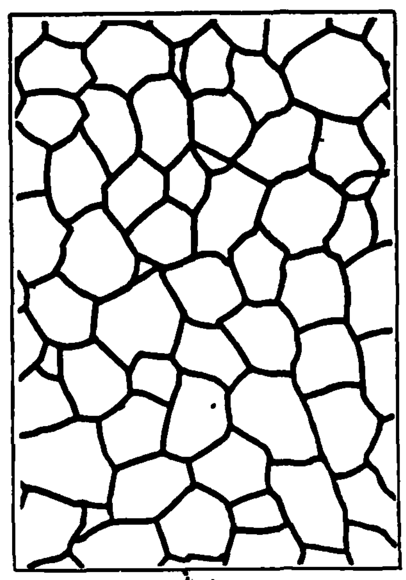

Grain Size No. 4

A.S.T.M. Tentative Grain Size Standards. Magnification X100.

E. References

References

1. A.J. Siegert and H. Goldstein, "Coherent and Incoherent Scattering from Assemblies of Scatterers", Appendix B, in Propagation of Sh.rt Radio Waves (e. D.E. Kerr), Vol. 13, M.I.T. Radiation Lab. Series, McGraw-Hill, 1948.
2. V.P. Glotov, "Coherent Scattering of Plane and Spherical Waves in Deep-Sea Layers Containing Discrete Inhomogeneities", Soviet Physics-Acoustics, Vol. 7, pp. 211-213, 1962. Translated from Doklady Akademia Nauk SSSR, Vol. 143, No. 2, pp. 312-315, 1962.
3. V.P. Glotov, "Coherent Scattering of Sound from Clusters of Discrete Inhomogeneities in Pulsed Emission", Soviet Physics-Acoustics, Vol. 8, pp. 220-222, 1963. Translated from Akusticheskii Zhurnal, Vol. 8, No. 3, pp. 281-284, July-September, 1962.
4. M. Arditi, F.S. Foster and J.W. Hunt, "Transient fields of Concave Annular Arrays", Ultrasonic Imaging, Vol. 3, pp. 37-61, (1981).
5. F. Oberhettinger, "On Transient Solutions of the Baffled Piston Problem", Journal of Research of NBS, Vol. 65B. No. 1, pp. 1-6, January-March 1961.

F. Appendix:

Echo Calculation for Piston-Point

Tranducer Pair

Appendix

Summary of equations used in the programs to follow that calculate the coherent term in eqt. 15.

for $c_t < a$ (c = sound velocity)

$$E_\delta(t) = 2\pi \int_{\rho=0}^{a} \int_{z=0}^{\frac{a}{2}} h(\rho,z,t)\ \rho d\rho dz$$

for ct > a

$$E_\delta(t) = 2\pi \int_{\rho=0}^{a} \int_{z=0}^{\frac{ct}{2}} h((\rho,z,t)\ \rho d\rho dz +$$

$$+ \int_{\rho=0}^{\frac{1}{2}ct+\frac{1}{2}a} \int_{z=0}^{\frac{ct}{2}[1-(\frac{a}{ct})^2]} h(\rho,z,t) \rho d\rho dz$$

where $h(\rho,z,t) = h(\vec{r},t)$ can be written as,

for case $\rho < a$

$$h(\vec{r},t) = 0 \qquad , \quad \frac{r}{c} > t-\frac{z}{c}$$

$$= \frac{c}{2\pi}\frac{1}{2} \qquad , \quad t-\frac{R'}{c} < \frac{r}{c} < t-\frac{z}{2}$$

$$= \frac{c}{2\pi^2 r} \quad \text{arc cos}\left[\frac{c^2(t-\frac{r}{c})^2-z^2+\rho^2-a^2}{2\rho\sqrt{c^2(t-\frac{r}{c})^2-z^2}}\right] \qquad , \quad t-\frac{R}{c} < \frac{r}{c} < \frac{R'}{2}$$

$$= 0 \qquad , \quad \frac{r}{c} < t-\frac{R}{c}$$

for case $\rho > a$

$$h(\vec{r},t) = 0 \qquad , \quad \frac{r}{c} > t-\frac{R'}{c}$$

$$= \frac{c}{2\pi^2 r} \quad \text{arc } c+j\left[\frac{c^2(t-\frac{r}{c})^2-z^2+\rho^2-a^2}{2\rho\sqrt{c^2(t-\frac{r}{c})^2-z^2}}\right] \quad , \quad t-\frac{R}{c} < \frac{r}{c} < \frac{R'}{2}$$

$$= 0 \quad , \quad \frac{r}{c} < t-\frac{R}{c}$$

where $r = \sqrt{\rho^2 + z^2}$

$$R = \sqrt{z^2 + (a+\rho)^2}$$

$$R' = \sqrt{z^2 + (a-\rho)^2}$$

e(t) is related to the radius a. It is easy to show that, if we let

$$t' = \frac{t}{a}$$

$$z' = \frac{z}{a}$$

$$\rho' = \frac{\rho}{a}$$

$$r' = \frac{r}{a}$$

$$R_a' = \frac{R'}{a}$$

$$R_a = \frac{R}{a}$$

then e(t) can be written as

$$e(t) = e'(t') \cdot a^2$$

where e'(t) is independent of a

When $t' \to o$, $e'(t') \to \frac{c^3 t'^2}{4}$

here $\frac{c^3 t'^2}{4}$ is the echo from scatterers uniformly distributed in a hemisphere due to an impulse exerted on a point-transmitter/infinite plane-reviewer transducer pair

when $t' \to \infty$, $e'(t') \to \frac{c}{4\pi}$

here $\frac{c}{4\pi}$ is the echo from scatterers uniformly distributed in half space due to an impulse exerted on a point-transmitter/point-receiver transducer pair.

Several computer programs are attached.

```
c-t     Edeltal.f

c       This program is used for calculating the impulse
c       response of a disc-point transducer pair
c       for the case when the time t < a/c
c       where a is the radius of the disc transducer and c the
c       velocity of sound in the medium . The program uses
c       subroutine DBLIN of the IMSL library.

        INTEGER IER
        real  DBLIN,F1,AX,AY,BX,BY,AERR,ERROR,C1
        EXTERNAL F1,AY,BY
        common /CI/a,c,t
        real  ar(400),swt(400)
        character *10 file

c       Parameter a is the radius of the disc transducer, c is the velocity
c       of sound in the medium and AERR the absolute error of the
c       calculation by the definition of the DBLIN subroutine.
c       The final calculated value of the impulse response is stored in
c       in an array named as ar while discrete time is stored in array swt.


c       When compiling & linking, type
c
c       f77 -o czc Edeltal.f /usr/lib/imsld.a

        a=1.25
        c=150000.0
        AERR=0.0001

c       write(6,10)
c10     format(4x,'Input t as starting time:')
c       read(5,20) t
c20     format(f16.12)
c       write(6,40)
c40     format(2x,'Input the name of the file to store the calculated data:')
c       read(5.60) file
c60     format(a10)
        t=0.000004893047
        open(unit=1,file='dataEE22',status='new',access='sequential',
     1  form='formatted')
        do 150 km=1,10
        t=t*1.05
        thr=a/c
        if(t .gt. thr .or. t .eq. thr) go to 111
        AX=0.0
        BX=a
        C1=DBLIN(F1,AX,BX,AY,BY,AERR,ERROR,IER)
        swt(km)=t
        ar(km)=C1
        write(1,202)swt(km),ar(km)
```

```
202     format(f16.12,f16.8)
        write(6,126) km,swt(km),ar(km)
126     format(10x,i5,3x,f16.12,3x,f16.8)
150     continue
        close(unit=1)
111     stop
        END

        REAL FUNCTION F1(x,y)
        real  x,y
        common /CI/a,c,t

c       To avoid the difficulty due to the inability of computer to deal
c       with the case where 0/0 appears in the calculation, we ignore a small
c       part of scatterers near the origin.

        rr=sqrt(x*x+y*y)
        R=sqrt(y*y+(a+x)*(a+x))
        Rp=sqrt(y*y+(a-x)*(a-x))
646     u=10000000000.0*(c*t-rr)*(c*t-rr)
        u=u-10000000000.0*y*y+10000000000.0*x*x-10000000000.0*a*a
        v=2.0*x*100000.0*sqrt(10000000000.0*(c*t-rr)*(c*t-rr)-10000000000.0*y*y)
648     if(rr .lt. 0.000125)go to 598
        ind=0
        jnd=0
        if(rr .gt. (c*t-R) .and. rr .lt. (c*t-Rp)) ind=5
        if(ind .eq. 5) F1=100000.0*x*c/(2.0*3.1416*3.1416*100000.0*rr)*acos(u/v)
        if(rr .gt. (c*t-y) .or. rr .eq. (c*t-y)) F1=0.0
        if(rr .gt. (c*t-Rp) .and. rr .lt. (c*t-y)) jnd=3
        if(jnd .eq. 3) F1=100000.0*x*c/(2.0*3.1416*rr*100000.0)
        if(rr .eq. (c*t-Rp)) F1=100000.0*x*c/(2.0*3.1416*rr*100000.0)
        if(rr .lt. (c*t-R) .or. rr .eq. (c*t-R)) F1=0.0
        go to 577
598     F1=0.0
577     RETURN
        END


        REAL FUNCTION AY(x)
        real  x
        AY=0.0
        return
        end

        REAL FUNCTION BY(x)
        real x
        common /CI/a,c,t

        BY=a/2.0
        return
        end
```

```
c-t     Edelta2.f

c       This program is used for calculating the impulse
c       response of a disk-point transducer pair
c       for the case when the time t > a/c
c       where a is the radius of the disc transducer and c the
c       velocity of sound in the medium . The program uses
c       subroutine DBLIN of the IMSL library.

        INTEGER IER
        double precision  DBLIN,F1,F2,AX,AY,BX,BY,AAY,BBY,AERR,ERROR,C1,C2
        EXTERNAL F1,F2,AY,BY,AAY,BBY
        common /CI/a,c,t
        double precision ar(400),swt(400)
        character *12 file

c       Parameter a is the radius of the disc transducer, c is the velocity
c       of sound in the medium and AERR the absolute error of the
c       calculation by the definition of the DBLIN subroutine. Since the
c       calculated value of impulse response for t> a/c is larger,
c       when setting  AERR equal to 10.0, the relative error is still
c       small enough to be accepted. The final calculated value of
c       the impulse reponse is stored in an array named as ar while discrete
c       time is stored in array swt.


c       When compiling & linking, type
c
c       f77 -o zcz Edelta2.f /usr/lib/imsls.a

        a=0.125
        c=150000.0
        AERR=0.1

c       write(6,10)
c10     format(4x,'Input t as starting time:')
c       read (5,20) t
c20     format(f16.12)
c       write(6,40)
c40     format(2x,'Input the name of the file to store the calculated data:')
c       read(5,50) file
c50     format(a12)
        t=0.0000701152661
        open(unit=1,file='datasal',status='new',access='sequential',
     1  form='formatted')
        do 150 km=1,20
        t=t*1.02
        AX=0.0
        BX=a
        C1=DBLIN(F1,AX,BX,AY,BY,AERR,ERROR,IER)
        AX=a
```

```
      BX=c*t/2.0+a/2.0
      swt(km)=t
      C2=DBLIN(F2,AX,BX,AAY,BBY,AERR,ERROR,IER)
      ar(km)=C1+C2
c     AERR=abs(ar(km)*0.01)
      write(1,202)swt(km),ar(km)
202   format(f16.12,f16.8)
      write(6,126) km,swt(km),ar(km)
126   format(10x,i5,3x,f16.12,3x,f16.8)
150   continue
      close(unit=1)
      stop
      END

      FUNCTION F1(x,y)
      double precision x,y,F1
      common /CI/a,c,t

c     To avoid the difficulty due to the inability of computer to deal
c     with the case where 0/0 appears in the calculation, we ignore a small
c     part of scatterers near the origin.

      rr=sqrt(x*x+y*y)
      R=sqrt(y*y+(a+x)*(a+x))
      Rp=sqrt(y*y+(a-x)*(a-x))
646   u=100000000.0*(c*t-rr)*(c*t-rr)
      u=u-100000000.0*y*y+100000000.0*x*x-100000000.0*a*a
      v=2.0*x*10000.0*sqrt(100000000.0*(c*t-rr)*(c*t-rr)-100000000.0*y*y)
648   if(rr .lt. 0.0000125)go to 598
      ind=0
      jnd=0
      if(rr .gt. (c*t-R) .and. rr .lt. (c*t-Rp)) ind=5
      if(ind .eq. 5) F1=10000.0*x*c/(2.0*3.1416*3.1416*10000.0*rr)*acos(u/v)
      if(rr .gt. (c*t-y) .or. rr .eq. (c*t-y)) F1=0.0
      if(rr .gt. (c*t-Rp) .and. rr .lt. (c*t-y)) jnd=3
      if(jnd .eq. 3) F1=10000.0*x*c/(2.0*3.1416*rr*10000.0)
      if(rr .eq. (c*t-Rp)) F1=10000.0*x*c/(2.0*3.1416*rr*10000.0)
      if(rr .lt. (c*t-R) .or. rr .eq. (c*t-R)) F1=0.0
      go to 577
598   F1=0.0
577   RETURN
      END


      FUNCTION F2(x,y)
      double precision  x,y,F2
      common /CI/a,c,t

      rr=sqrt(x*x+y*y)
      R=sqrt(y*y+(a+x)*(a+x))
      Rp=sqrt(y*y+(a-x)*(a-x))
      u=100000000.0*(c*t-rr)*(c*t-rr)
      u=u-100000000.0*y*y+100000000.0*x*x-100000000.0*a*a
```

```
      v=2.0*x*10000.0*sqrt(100000000.0*(c*t-rr)*(c*t-rr)-100000000.0*y*y)
      knd=0
      if(rr .gt. c*t-R .and. rr .lt. c*t-Rp) knd=8
      if(knd .eq. 8) F2=10000.0*x*c/(2.0*3.1416*3.1416*rr*10000.0)*acos(u/v)
      if(rr .gt. (c*t-Rp) .or. rr .eq. (c*t-Rp)) F2=0.0
      if(rr .lt. (c*t-R) .or. rr .eq. (c*t-R)) F2=0.0
689   RETURN
      END

      FUNCTION AY(x)
      double precision  x,AY
      AY=0.0
      return
      end

      FUNCTION BY(x)
      double precision  x,BY
      common /CI/a,c,t

      BY=c*t/2.0
      return
      end


      FUNCTION AAY(x)
      double precision  x,AAY

      AAY=0.0
      return
      end

      FUNCTION BBY(x)
      double precision  x,BBY
      common /CI/a,c,t

      BBY=c*t/2.0*(1.0-a*a/(c*c*t*t))
      return
      end
```

```
c-t     joindata.f

c       Programs Edelta2 or Edeltal might stop being executed while
c       they are supposed to be. The reason can be the singularity
c       or ill behaviour(not smooth enough according to the request of
c       given error) of the integrand. The easy way to get rid of
c       such difficulty is to jump over these points where the
c       integrand doesn't behave well. It will not do harm to our
c       calculation because such points are not continuous. From the
c       point of view of physics, the calculated curve should be
c       continuous.  This Program joindata.f is used to join separated
c       data files together to produce a final data file.

        real swt(1000),ar(1000)
        character*8 file
        character*1 q,qq,qqq,q4,q5



        nor=1
77      write(6,1000)
1000    format(2x,'Do you want to read some data file ? y/n?')
        read(5,1010) q
1010    format(al)
        if(q .eq. 'n') go to 1045
        write(6,11)
11      format(2x,'Input the name of the file:')
        read(5,14) file
14      format(a8)
        write(6,1020)
1020    format(2x,'How many records does the file have?')
        read(5,1030) norl
        nom=nor+norl-1
1030    format(i4)
        open(unit=1,file=file,status='old',access='sequential',
     1  form='formatted')
        do 100 i=nor,nom
        read(1,15)swt(i),ar(i)
15      format(f16.8,f16.8)
        write(6,10)i, swt(i),ar(i)
10      format(4x, i4,f16.8,f16.8)
100     continue
        close(unit=1)
        nor=nom+1
        go to 77

1045    write(6,1055)
1055    format(3x,'Do you want to type in some data? y/n?')
        read(5,1205)q5
1205    format(al)
        if(q5 .eq. 'n') go to 1095
        nor=nor-1
```

```
1050    write(6,1200)
1200    format(3x,'will t automatically be calculated? y/n?')
        read(5,1210) qqq
1210    format(a1)
        if(qqq .eq. 'n') go to 1250
        write(6,1212)
1212    format(2x,'Is this the first value of t? y/n?')
        read(5,1215) q4
1215    format(a1)
        if(q4 .eq. 'n') go to 1265
        write(6,1260)
1260    format(2x,'Input previous t as initial value:')
        read(5,1270) t
        if(q4 .eq. 'y') t=t*1.002*1.002
1265    nor=nor+1
1270    format(f16.12)
        t=t*1.002
        write(6,1275)t
1275    format(f16.8)
        write(6,1280)
1280    format(4x,'Input echo(t):')
        read(5,1290) ar(nor)
1290    format(f16.8)
        swt(nor)=t
        go to 108
1250    nor=nor+1
        write(6,1060)
1060    format(2x,'Input t & echo(t):')
        read(5,1070) swt(nor),ar(nor)
1070    format(f16.12,f16.8)
108     write(6,1080)
1080    format(2x,'Do you think you already input all data? y/n?')
        read (5,1090) qq
1090    format(a1)
        if(qq .eq. 'n') go to 1050
1095    nor=nor-1
        write(6,1100)nor
1100    format(5x,'The No. of records of the new file is :',i5)
        open(unit=1,file='CTF12data',status='new',access='sequential',
     1  form='formatted')
        do 1150 j=1,nor
        write(1,1110)swt(j),ar(j)
1110    format(f16.8,f16.8)
1150    continue
        stop
        end
```

```
c-t     planepoint.f

c       This program is used to calculate the echo from scatterers
c       which are uniformly distributed in half space due to the
c       impulse input to infinite plane-point transducer pair. The
c       calculated data can serve as a comparison with the calculated
c       result by program Edeltal.fi. Note the data is normalized here
c       by being divided by 2.0*3.1416.

        character*6 file


        write(6,11)
11      format(2x,'input the name of the file:')
        read(5,14)file
14      format(a6)
        open(unit=1,file=file,status='new',access='sequential',
     1  form='formatted')
        t=0.0000001
        do 100 i=1,450
        t=1.01*t
        f=150000.0*150000.0*150000.0*t*t/(4.0*2.0*3.1416)
        write(1,20) t,f
20      format(f16.12,f16.8)
100     continue
        close(unit=1)

        stop
        end
```

```
c-t     curvefit.f


        real swt(1000),ar(1000),aa(1000),rna(5)
        character*12  file,file1,file2


        write(6,30)
30      format(4x,'Input the name of the file:')
        read(5,40) file
40      format(a12)
        open(unit=1,file=file,status='old',access='sequential',
     1  form='formatted')
        do 10 i=1,387
        read(1,20) swt(i),ar(i)
20      format(f16.12,f16.8)
10      continue
        close(unit=1)

        write(6,70)
70      format(2x,'Input the name of the new file to store the fitting curve:')
        read(5,80) file1
80      format(a12)

        write(6,72)
72      format(4x,'Input the name of the new file to store the estimates:')
        read(5,80) file2

c       Input the initial value of amp, sigma & cst as curve fitting paremeters

        write(6,50)
50      format(4x,'Input the initial value for amp,sigma & cst :')
        read(5,60) amp,sigma,cst
60      format(f20.10,f20.10,f20.10)

        de=1.0
        all=1.0
        rin=0.001


c       curve fitting for estimating amp,sigma & cst

        call difference(amp,sigma,cst,swt,ar,e,aa)
380     ampl=amp-0.01
        sigmal=sigma-0.01
        cstl=cst-0.01
        call difference(ampl,sigma,cst,swt,ar,ea,aa)
        call difference(amp,sigmal,cst,swt,ar,es,aa)
        call difference(amp,sigma,cstl,swt,ar,ec,aa)
        ga=(e-ea)/0.01
        gs=(e-es)/0.01
        gc=(e-ec)/0.01
```

```
      adl=amp-all*ga
      sdl=sigma-all*gs
      cdl=cst-all*gc
      call difference(adl,sdl,cdl,swt,ar,el,aa)
      if (e .lt. el) go to 390
      al2=all*1.3
      ad2=amp-al2*ga
      sd2=sigma-al2*gs
      cd2=cst-al2*gc
      call difference(ad2,sd2,cd2,swt,ar,e2,aa)
370   if(e2 .gt. el) go to 360
      el=e2
      all=al2
      al2=all*1.3
      ad2=amp-al2*ga
      sd2=sigma-al2*gs
      cd2=cst-al2*gc
      call difference(ad2,sd2,cd2,swt,ar,e2,aa)
      go to 370

360   e2=el
      al2=all
      all=0.618*al2
      adl=amp-all*ga
      sdl=sigma-all*gs
      cdl=cst-all*gc
      call difference(adl,sdl,cdl,swt,ar,el,aa)
400   if(el .gt. e) go to 390

      de=abs(e-el)
      rna(1)=rna(2)
      rna(2)=rna(3)
      rna(3)=rna(4)
      rna(5)=de
      srna=rna(1)+rna(2)+rna(3)+rna(4)+rna(5)
      if(srna .lt. rin) go to 130
      e=el
      amp=adl
      sigma=sdl
      cst=cdl
      go to 380

390   e2=el
      al2=all
      all=al2*0.618
      adl=amp-all*ga
      sdl=sigma-all*gs
      cdl=cst-all*gc
      call difference(adl,sdl,cdl,swt,ar,el,aa)
      go to 400

130   open(unit=1,file=file2,status='new',access='sequential',
     1 form='formatted')
```

```
      write(1,160) amp,sigma,cst
160   format(f20.12)
      close(unit=1)

c     Create new data file to be displied

      open(unit=1,file=file1,status='new',access='sequential',
     1 form='formatted')
      do 90 jmm=1,387
      write(1,100)swt(jmm),aa(jmm)
100   format(f16.12,f16.8)
90    continue
      close(unit=1)

      write(6,137)
137   format(2x,'The end.')

      stop
      end


      subroutine difference(AMP,SIGMA,CST,SWT,AR,E,AA)

      REAL AR(1000),AA(1000),SWT(1000)

      E=0.0
      DO 200 KK=1,387
      AA(KK)=AMP*EXP(-1.0*SIGMA*SWT(KK))+CST
      E=E+ABS(AA(KK)-AR(KK))
200   CONTINUE
      RETURN
      END
```

G. Group Publications Relevant to this Research

Papers

J. Saniie, E.S. Furgason and V.L. Newhouse, "Ultrasonic Imaging through Reverberant Thin Layers," Materials Evaluation, Vol. 40, pp. 115-124, 1982.

V.L. Newhouse, N.M. Bilgutay, J. Saniie and E.S. Furgason, "Flaw to Grain Echo Enhancement by Split-Spectrum Processing," Ultrasonics, Vol. 20, pp. 59-68, 1982.

V.L. Newhouse and I. Amir, "Use of an Ellipsoidal Mirror to Minimize Multipath and Scattering Effects in Gap Measurement between Rough Cylindrical Surfaces," Materials Evaluation, Vol. 40, No. 7, pp. 762-769, 1982.

I. Amir, N.M. Bilgutay, and V.L. Newhouse, "Analysis and Comparison of Some Frequency Compounding Algorithms for the Reduction of Ultrasonic Clutter". Accepted for publication by IEEE Trans. on Sonics and Ultrasonics.

V.L. Newhouse and I. Amir, "On the Creation of a Coherent Echo from Random Media." Submitted for publication in Ultrasonic Imaging.

Conference Presentations

V.L. Newhouse and S. Tartono, "A Proposed Technique for the Statistical Analysis of Texture", Seventh International Symposium on Ultrasonic Imaging and Tissue Characterization, Gaithersburg, MD, June 6-9, 1982.

V.L. Newhouse, "Statistical Texture Analysis" at Fourth Annual IEEE Conference on Frontiers of Engineering in Health Care, Phila., PA, September 20-21, 1982.

I. Amir and V.L. Newhouse, "The Separation of Coherent Echoes from Sub-Wavelength Scatterers." Invited paper presented at the AIUM Conference, New York, 1983.

V.L. Newhouse, I. Amir and Y. Guoyao, "On the Creation of a Coherent Echo from Random Media," 1984 IE^3 Ultrasonics Symposium, Dallas, TX.

I. Amir, V.L. Newhouse and N. Bilgutay, "Theoretical Analysis and Performance of the Minimization Algorithm and Comparison with Conventional Techniques," Presented at 3rd European Conference on Nondestructive Testing, Florence, October 1984.

I. Amir and N. Bilgutay, "Theoretical Analysis and Performance of the Minimization Algorithm." To be presented at the Eleventh World Conference on Nondestructive Testing, November 1985, Las Vegas, Nevada.

END

FILMED

7-85

DTIC